EasyChair Preprint

№ 5671

CFD Investigation of Falling Film Flow over Horizontal Tube

Furqan Tahir, Abdelnasser Mabrouk and Muammer Koc

June 3, 2021

CFD Investigation of Falling Film Flow over Horizontal Tube

[1*]Furqan Tahir, [1,2]Abdelnasser Mabrouk, [1]Muammer Koç
[1] Division of Sustainable Development (DSD), College of Science & Engineering (CSE), Hamad Bin Khalifa University (HBKU), Education City, P.O. Box 34110, Qatar
[2] Qatar Environment and Energy Research Institute (QEERI), Hamad Bin Khalifa University (HBKU), Education City, P.O. Box 34110, Qatar

* E-mails: futahir@hbku.edu.qa

Abstract
The heat exchangers employed in multi-effect desalination (MED) and ammonia/lithium bromide refrigeration systems are usually of falling film types. In horizontal falling film exchangers, liquid is sprayed on the top of bundle, which forms thin film around the tube that makes these exchangers to operate at low temperature difference and spray density. The film hydrodynamics around the tube affects the heat and mass transfer mechanisms, which causes heat exchanger performance to change. In this work, a 2D computational fluid dynamics (CFD) model has been developed in Ansys fluent v18.0, to understand falling film dynamics around the tube of 25.4 mm diameter. The physical domain consists of two tubes with an impingement height of 15.9 mm and inter-tube spacing of 31.8 mm. For water entrance, 2 mm orifice is selected at the top of first tube. The spray density is varied from 0.02-0.05 kg/(m·s) to examine film thickness and residence time for first and second tube. The CFD results shows that the film thickness increases with the increasing spray density, the average film thickness rises by 56% and time for complete wetting decreases by 48.6% ,when the spray density increases from 0.02 to 0.05 kg/(m·s). In addition, the average film thickness reduces by around 13.7% for second tube as compared to that of first tube because of impingement height difference.

Keywords: CFD, Falling Film, Horizontal Tube, Hydrodynamics

I. Introduction

The horizontal tube falling film evaporators are commonly used in multi-effect desalination (MED) plants as these evaporators exhibit high heat transfer coefficient as compared to flooded exchangers [1–3]. The heat transfer coefficient of falling film evaporators strongly affects by film distribution and hydrodynamics [4–8]. The film thickness around the tube is studied experimentally and numerically by many researchers [9,10] and the film distribution is influenced by many factors such as thermophysical properties, wall adhesion, tube layout and operating conditions [11–13]. In 1916, Nusselt [14] proposed a film thickness δ correlation as shown in Eq. (1) by assuming negligible inertial effects.

$$\delta = \sqrt[3]{\frac{3\mu_l\Gamma_{1/2}}{\rho_l(\rho_l-\rho_g)g\sin\theta}} \quad (1)$$

where $\Gamma_{1/2}$ is spray density, θ is inclination angle, μ_l is liquid viscosity, ρ_l is liquid density, ρ_g is gaseous phase density and g is acceleration due to gravity. From Eq. (1), it is clear that film distribution is symmetric across the upper and lower half of tube surface. Hou et al. [15] performed experiments and observed that the film distribution is asymmetric and also it is affected by tube diameter d and inter-tube spacing s. They modified the Eq. (1) as shown in Eq. (2), by introducing s/d factor and constant C and n for asymmetric profile fit, which are different for upper and lower half of tube.

$$\delta = C \cdot \sqrt[3]{\frac{3\mu_l\Gamma_{1/2}}{\rho_l(\rho_l-\rho_g)g\sin\theta}} \left(\frac{s}{d}\right)^n \quad (2)$$

Ji et al. [16] conducted numerical experiments and found the minimum thickness at θ=120° and they proposed modification in Eq. (1) by replacing θ by 0.75θ for better film thickness prediction. Tahir et al. [17,18] analyzed the effect of thermophysical properties on film distribution and they concluded that the fluid with surface tension and viscosity results in increased conductive thermal resistance which may deteriorate heat transfer performance. In the literature, the influence of inter-tube spacing has been reported however, its effect on residence time is lacking. In the present work, impact of impingement height (15.9 mm for first tube and 31.8 mm for second tube) on film distribution has been analyzed. The film distribution and residence time for first and second tube with respect to spray density has been quantified and discussed.

II. Computational Fluid Dynamics (CFD) model

Fig. 1a shows the CFD domain and boundary conditions, consisting of two tubes of 25.4 mm with 2 mm orifice for water entrance. The thermophysical properties of water and air are computed at 20 °C. As the nature of the problem is symmetric, therefore only half of the domain is selected for computation. It is assumed that the flow is laminar and adiabatic, there is no vapor flow and tube wall is super hydrophilic to ensure complete wetting of tubes [19]. The domain is meshed with quad dominant elements with fine boundary layers on the tube wall as shown in Fig.1b,

for accurate capturing of liquid-gas interface.

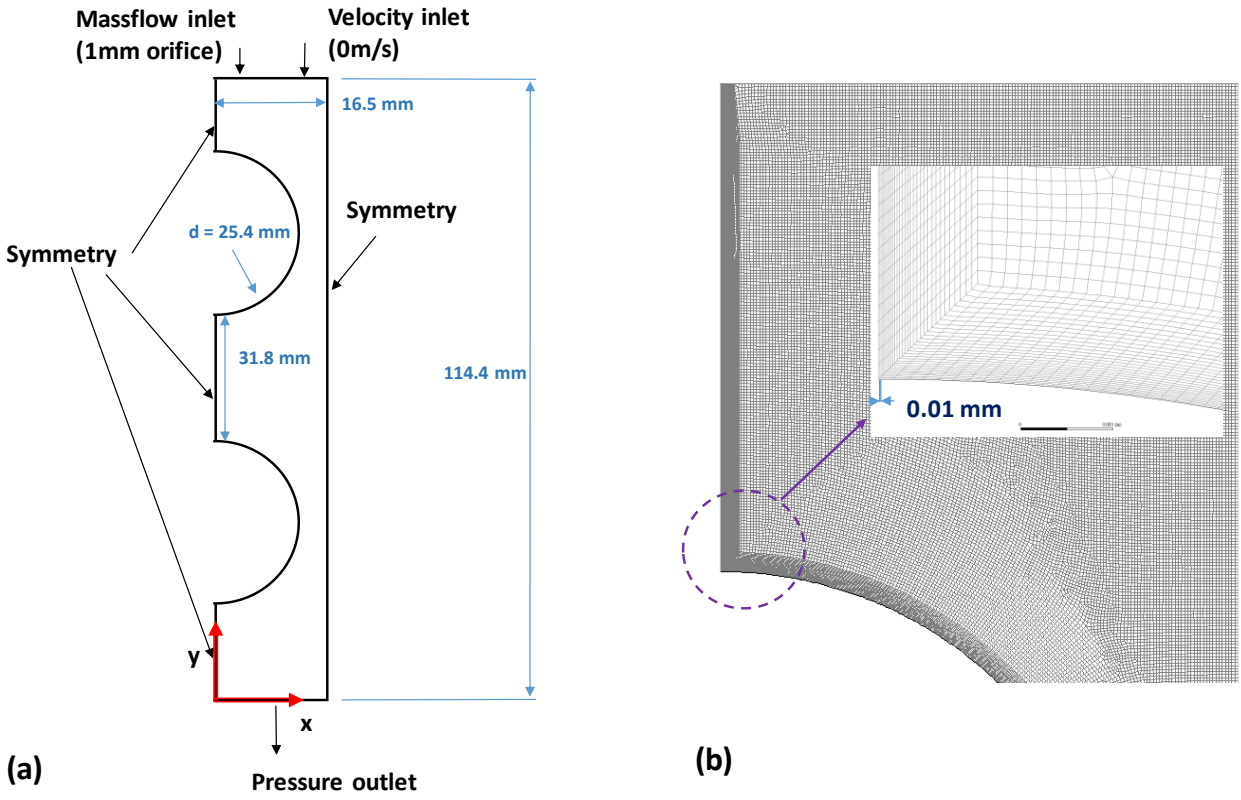

Fig. 1: (a) CFD domain with boundary conditions and (b) Mesh with fine boundary layers near to tube wall

The conservation of mass and momentum are discretized and solved for each phase, as per volume of fluid (VOF) model shown in Eq. 3. The VOF model is widely used where liquid-gas interfaces are distinct [20].

$$\frac{\partial(\alpha_i \rho_i)}{\partial t} + \nabla \cdot \left(\alpha_i \rho_i \overrightarrow{V_i}\right) = 0 \qquad (i = g \ \ or \ \ l) \tag{3}$$

where V is velocity, α is void fraction and g/l denotes gas/liquid phases. The thermophysical property is computed by:

$$\beta = \alpha_l \beta_l + (1 - \alpha_l)\beta_g \tag{4}$$

where β is any thermophysical property. The spray density $\Gamma_{1/2}$ has been varied from 0.02-0.05 kg/(m·s), which corresponds to droplet to jet mode. The detailed methodology, solver settings and validation details can be found in [17].

III. Results and discussion

Fig.2a shows water film thickness around the tube surface and it can be seen that the film thickness in the impingement and detachment region is higher than other region. As the liquid hits the surface at top, it disperses in to circumferential direction, and with the continuous influx, a thicker region is formed. In addition, as the liquid reaches at the bottom, it starts to compile due to surface tension and viscous force and detaches when it overcomes the gravitational force. The accumulation of liquid phase at the bottom results in higher time-averaged thickness. Due to higher thickness at the top and bottom, average film thickness has been computed from θ = 20°-160° for comparison purpose as shown in Fig. 2b. With the rise in spray density from 0.02 to 0.05 kg/(m·s), the average film thickness increases by 56% and 61% for the first and second tube respectively. At 0.02 and 0.05 kg/(m·s), the average film thickness for the second tube is 14.4% and 11.5% less than that of first tube, respectively.

Fig 3a and b shows the volume fraction contours for top and bottom tubes at t = 0.9 s and $\Gamma_{1/2}$ = 0.05 kg/(m·s). As the spray density of 0.05 kg/(m·s) corresponds to jet-mode, the continuous liquid stream can be observed after the first tube. At t = 0.9 s, the second tube is completely wet and liquid gathers at the bottom of tube which forms continuous stream after detachment. The residence time, which can be deduced from time for complete wetting of tubes, is shown in Fig 3c, for different operating conditions. The time required to cover the first tube at $\Gamma_{1/2}$ = 0.02 kg/(m·s) is 0.66 s, which decreases as the film average velocity increases because of rise in spray density. The

time to cover tube decreases by 48.6% when the spray density rises from 0.02 to 0.05 kg/(m·s). Similarly, the time for complete wetting of second tube at 0.02 kg/(m·s) is 1.62 s, which reduces to 0.87 s at 0.05 kg/(m·s). This trend implies that at higher spray densities, the contact time for heat transfer with the tube surface is lowered, which may results in reduced heat transfer coefficient. This is one of the reason that heat transfer coefficient for droplet mode (low spray density) is higher the jet mode (high spray density) [21].

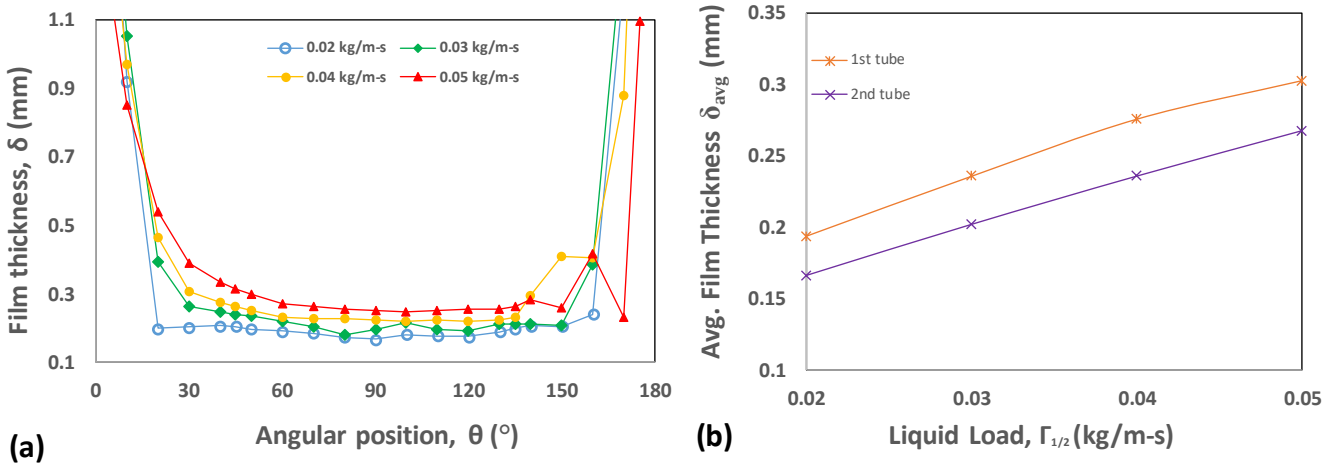

Fig. 2: (a) Film thickness distribution around first tube surface for different spray densities and (b) average film thickness (from θ = 20°-160°) with respect to spray densities

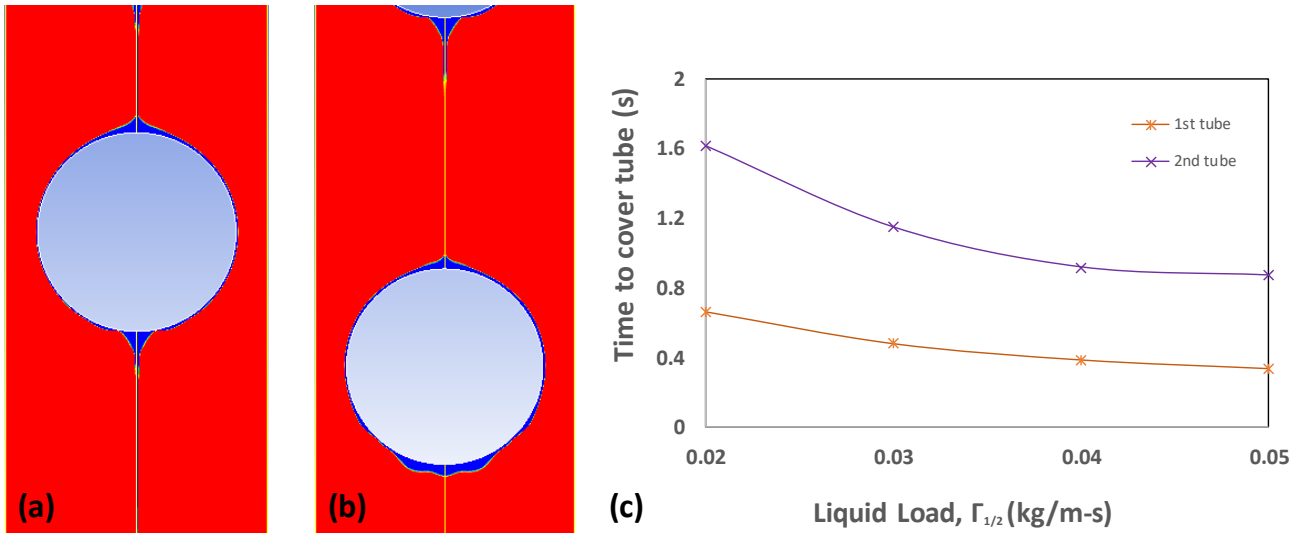

Fig. 3: Wetting of (a) first and (b) second tube at $\Gamma_{1/2}$ = 0.05 kg/(m·s) and t = 0.9 s, and (b) time to complete wetting of first and second tubes with respect to spray densities

IV. Conclusions

A two-dimensional computational fluid dynamics (CFD) model for analyzing falling film hydrodynamics has been presented. Two tubes of 25.4 mm diameter with an impingement height of 15.9 mm and tube-to-tube spacing of 31.8 mm has been selected, to examine the effect of spray density and impingement height on the falling film thickness and the time for the complete wetting of first and second tube. The numerical results shows that the falling film thickness at the impingement and detachment regions, is very high as compared to the other region (θ = 20° - 160°). The average film thickness grows by 56 % and 61 % for the first and second tube, respectively, when the spray density is changed from 0.02 to 0.05 kg/(m·s). The average film thickness decreases by 13.7% for the second tube as that of the first tube due to the impingement height difference. Furthermore, the time for complete wetting of tubes decreases by 48 % for the first tube due to the increased average velocity and the higher spray density. At low spray density (droplet mode), the lower average film thickness that reflects lower conduction thermal resistance and higher residence time, may lead to better heat transfer performance when compared to that of higher spray density (jet mode).

References

[1] F. Tahir, A. Mabrouk, M. Koc, Review on CFD analysis of horizontal falling film evaporators in multi effect desalination

plants, Desalin. Water Treat. 166 (2019) 296–320. doi:10.5004/dwt.2019.24487.

[2] F. Tahir, A.A. Mabrouk, M. Koc, CFD analysis of spray nozzle arrangements for multi effect desalination evaporator, Proceeding 3rd Therm. Fluids Eng. Conf. (2018) 935–941. doi:10.1615/TFEC2018.fip.021685.

[3] A. Mabrouk, A. Abotaleb, F. Tahir, M. Darwish, R. Aini, M. Koc, A. Abdelrashid, High Performance MED Desalination Plants Part I: Novel Design MED Evaporator, in: IDA 2017 World Congr. Water Reuse Desalin., Sao Paulo, Brazil, 2017.

[4] A. Karmakar, S. Acharya, Wettability Effects on Falling Film Flow and Heat Transfer Over Horizontal Tubes in Jet Flow Mode, J. Heat Transfer. 142 (2020). doi:10.1115/1.4048088.

[5] A. Karmakar, S. Acharya, Wettability Effects on Falling Film Heat Transfer Over Horizontal Tubes in Jet Flow Mode, in: ASME 2019 Heat Transf. Summer Conf., American Society of Mechanical Engineers, 2019. doi:10.1115/HT2019-3532.

[6] B. Narváez-Romo, J.R. Simões-Moreira, Falling Liquid Film Evaporation in Subcooled and Saturated Water Over Horizontal Heated Tubes, Heat Transf. Eng. 38 (2017) 361–376. doi:10.1080/01457632.2016.1189275.

[7] G. Ribatski, A.M. Jacobi, Falling-film evaporation on horizontal tubes—a critical review, Int. J. Refrig. 28 (2005) 635–653. doi:10.1016/j.ijrefrig.2004.12.002.

[8] F. Tahir, A. Mabrouk, M. Koc, Heat Transfer Performance of Falling Film Evaporators Used in Multi Effect Desalination (MED) Plants, in: 1st Int. Conf. Sustain. Energy-Water-Environment Nexus Desert Clim. Doha, Qatar, 2019.

[9] Q. Qiu, X. Zhu, L. Mu, S. Shen, Numerical study of falling film thickness over fully wetted horizontal round tube, Int. J. Heat Mass Transf. 84 (2015) 893–897. doi:10.1016/j.ijheatmasstransfer.2015.01.024.

[10] X. Chen, S. Shen, Y. Wang, J. Chen, J. Zhang, Measurement on falling film thickness distribution around horizontal tube with laser-induced fluorescence technology, Int. J. Heat Mass Transf. 89 (2015) 707–713. doi:10.1016/j.ijheatmasstransfer.2015.05.016.

[11] F. Tahir, A. Mabrouk, M. Koc, CFD Analysis of Falling Film Wettability in MED Desalination plants, in: Qatar Found. Annu. Res. Conf. Proc., 2018: p. EEPD650. doi:10.5339/qfarc.2018.EEPD650.

[12] A. Mabrouk, A. Abotaleb, H. Abdelrehim, F. Tahir, M. Koc, A. Abdelrashid, A. Nasralla, HP MED Plants, Part II: Novel Integration MED-Absorption Vapor Compression, in: IDA 2017 World Congr. Water Reuse Desalin., Sao Paulo, Brazil, 2017.

[13] F. Tahir, Computational Fluid Dynamics (CFD) Analysis of Horizontal Tube Falling Film Evaporators Used in Multi Effect Desalination (MED) Plant, Hamad Bin Khalifa University, 2020.

[14] W. Nusselt, Die oberflachenkondensation des wasserdamphes, VDI-Zs. 60 (1916) 541–546.

[15] H. Hou, Q. Bi, H. Ma, G. Wu, Distribution characteristics of falling film thickness around a horizontal tube, Desalination. 285 (2012) 393–398. doi:10.1016/j.desal.2011.10.020.

[16] G. Ji, J. Wu, Y. Chen, G. Ji, Asymmetric distribution of falling film solution flowing on hydrophilic horizontal round tube, Int. J. Refrig. 78 (2017) 83–92. doi:10.1016/j.ijrefrig.2017.03.022.

[17] F. Tahir, A. Mabrouk, M. Koç, Impact of surface tension and viscosity on falling film thickness in multi-effect desalination (MED) horizontal tube evaporator, Int. J. Therm. Sci. 150 (2020) 106235. doi:10.1016/j.ijthermalsci.2019.106235.

[18] F. Tahir, A. Mabrouk, M. Koç, CFD Analysis of Falling Film Hydrodynamics for a Lithium Bromide (LiBr) Solution over a Horizontal Tube, Energies. 13 (2020) 307. doi:10.3390/en13020307.

[19] S.A. Khan, F. Tahir, A.A.B. Baloch, M. Koc, Review of Micro–Nanoscale Surface Coatings Application for Sustaining Dropwise Condensation, Coatings. 9 (2019) 117. doi:10.3390/coatings9020117.

[20] A. Baloch, H. Ali, F. Tahir, Transient Analysis of Air Bubble Rise in Stagnant Water Column Using CFD, in: ICTEA Int. Conf. Therm. Eng., 2018.

[21] S.M. Hosseinnia, M. Naghashzadegan, R. Kouhikamali, CFD simulation of water vapor absorption in laminar falling film solution of water-LiBr ─ Drop and jet modes, Appl. Therm. Eng. 115 (2017) 860–873. doi:10.1016/j.applthermaleng.2017.01.022.